Preprints of the 19th World Congress
The International Federation of Automatic Control
Cape Town, South Africa. August 24-29, 2014

Hydrogen Separation Via a Palladium Membrane: Modeling and Identification ⋆

S. Bittanti * **L. Bolzani** ** **S. Canevese** *** **A. De Marco** ****
F. Drago *** **P. Pinacci** ***

* *IFAC Fellow; Department of Electronics, Information Technology and Bioengineering (DEIB), Politecnico di Milano, Milan, Italy (e-mail: bittanti@elet.polimi.it)*
** *Former student, Politecnico di Milano, Milan, Italy (e-mail: luca.bolzani@yahoo.it)*
*** *RSE S.p.A., Milan, Italy (e-mail: {canevese, drago, pinacci}@rse-web.it)*
**** *Process engineer, Milan, Italy (e-mail: antoniodemarco65@gmail.com)*

Abstract: Palladium membranes can be effectively employed inside reactors for Water-Gas Shift (WGS, namely $CO + H_2O \rightleftarrows CO_2 + H_2$), to separate hydrogen from the products, thus increasing the reaction conversion at the same time. Driven by its own partial pressure difference on the two sides of palladium, hydrogen permeates across the membrane up to the reactor lumen, from where it is pushed towards the outlet thanks to a sweep gas.
A control-oriented dynamic model has been set up, accounting for the permeation characteristics of palladium and of the underlying porous support layer and for the presence of the sweep gas. The main uncertain parameters in the model have been identified from laboratory experiments, carried out on two membranes and on a WGS reactor equipped with one of them.

Keywords: Hydrogen permeation; palladium membranes; dynamic modelling; parameter identification; water-gas shift reactor.

1. INTRODUCTION

As is well known, the conversion of CO into CO_2 via H_2O, namely the *Water-Gas Shift reaction* (WGS), leads to the generation of H_2:

$$CO + H_2O \rightleftarrows CO_2 + H_2, \quad \Delta H^0_{298K} = -41 kJ/mol. \quad (1)$$

The reaction rate can be increased by inserting a palladium (Pd) membrane into the reactor (Kikuchi (1995), Buxbaum and Kinney (1996), Gallucci et al. (2013), Lu et al. (2007), Augustine et al. (2011)). H_2 permeates through the Pd lattice, thanks to the difference between its partial pressures on the two sides of the membrane, whereas the remaining gases are blocked. With a flow of inert gas on the outlet side, H_2 can be swept out of the reactor and collected. The reaction rate depends upon the flow of the swept H_2; thus, it can be controlled by modulating the sweep gas flow.

Palladium membranes can also be employed in a number of other reactors, *e.g.* in reformer reactors for the production of H_2, in order to separate H_2 from the reaction products (Kikuchi (1995), Shirasaki et al. (2009)): almost pure H_2 flows across the membrane to the reactor lumen, and can then be extracted by a suitable extractor, such as a blower.

These different kinds of reactor can operate in a variety of complex processes, ranging from coal-fed integrated gasification combined cycles to purified bio-methane production by biogas upgrading. Accurate control of the operating conditions of each device contributes to increasing the whole plant efficiency and/or the quality of the produced gases. A detailed model of a membrane enhancing a reactor action, in turn, is helpful for the reactor control design, with a benefit for the overall process.

In this paper, we construct a control-oriented model of a Pd membrane complemented with its structural support. The proposed model is calibrated thanks to experimental data collected on a laboratory plant at RSE (Ricerca sul Sistema Energetico) in Milan, Italy. The test rig (Pinacci and Drago (2012), Pinacci et al. (2010)) can operate up to 30 bar and 450 °C and it includes process gas feeding units, for CO, CO_2, H_2, N_2, He and steam; a sweep gas feeding unit; a tubular electric oven, for temperature control, to host a membrane or a reactor - a WGS reactor for this work - for testing; cooling lines for the membrane or reactor outlet gases, to condense steam and thus to allow to determine the gas composition by a gas-chromatographer; a computer, interfaced to a controller and a data acquisition system for the main process variables (temperature, pressure, flow rate).

⋆ This work has been financed by the Research Fund for the Italian Electrical System under the Contract Agreement between RSE S.p.A. and the Ministry of Economic Development - General Directorate for Nuclear Energy, Renewable Energy and Energy Efficiency in compliance with the Decree of March 8, 2006. The support by the MIUR national project "Identification and adaptive control of industrial systems" and by CNR - IEIIT is also gratefully acknowledged.

The paper is organized as follows: Sections 2 and 3, respectively, report the proposed model for the membrane and the model of a catalytic WGS reactor; identification of the membrane model parameters is dealt with in Section 4; Section 5 reports simulation results for the overall membrane reactor model.

2. SUPPORTED MEMBRANE MODEL

The working mechanism of a Pd membrane can be described as follows, with reference to its cross section. A gas mixture including H_2 flows on the *feedgas side* of the membrane. Due to difference in partial pressure across the membrane, H_2 is pushed towards the membrane surface, where it is absorbed and dissociates so that it can be permeated across the Pd lattice. Then, when hydrogen atoms reach the other side of the membrane, the *permeate side* or *sweep gas side*, they associate again and are desorbed from the membrane surface. Finally, they are swept away to the process outlet by an inert sweep gas (nitrogen in the tests considered in this work), which is often in counter current with respect to the feedgas.

A Pd membrane can be inserted in a chemical reactor, so the *feedgas side* is also called the *reactor side*. An axial section of a packed-bed catalytic membrane reactor with a layered tubular structure is reported in Fig. 1. Since the reactor adopted here for the membrane model verification is a catalytic shift reactor, the chemical species in the figure are the reactants and products of the WGS reaction (1). Therefore, in this case the membrane feedags is composed of CO, CO_2, H_2 and steam.

The reactor is made up of coaxial cylindric regions: an outer steel cylinder (steel wall) contains highly porous catalyst pellets, where the reaction takes place; between the catalyst zone and the internal lumen, there is a cylindric composite membrane, made of Pd layers deposited on a porous stainless steel support and permeable to H_2. The membrane ensures H_2 separation from the gas mixture flowing through the pellet region: this way, the reaction efficiency is enhanced (equilibrium is shifted towards the products) and pure H_2 (or H_2 and N_2, if this latter is used as a sweep gas) is obtained in the lumen. For the WGS reaction, in particular, a mixture of CO_2 and steam, with very small CO residuals, is also obtained at the reactor outlet: thus, in case the final goal is CO_2 sequestration, it is enough to condense water to have pure CO_2.

Thanks to cylindric symmetry (see Fig. 1), the reference coordinate for the *whole membrane reactor model* is the axial coordinate z: the membrane reactor length l is divided into N strips, *i.e.* into N control volumes, and mass and energy conservation equations are written in each k-th strip (Δz long). Such equations account for mass and energy fluxes along z and along the radial direction. The proposed model for the membrane is dealt with in Sections 2.1-2.4. The reactor model is briefly discussed in Section 3.

2.1 H_2 Permeation through the Pd Membrane

For a membrane with no defects, the gas flux across the Pd membrane is composed of H_2 only, and H_2 permeation across the Pd layers can be described by the Sieverts

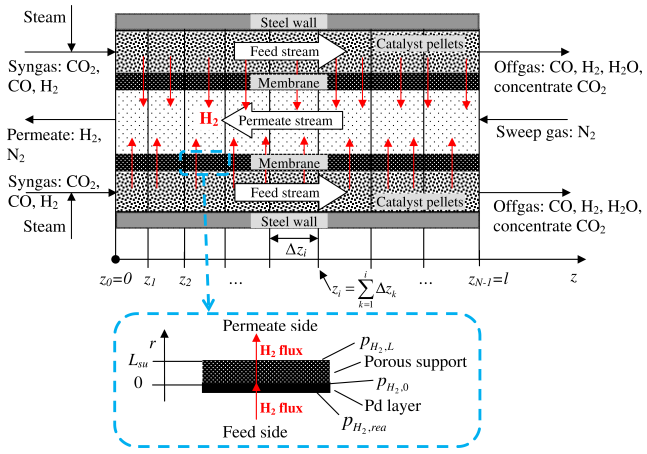

Fig. 1. Top: reactor axial section, with the main gaseous fluxes; bottom: zoom on the supported Pd membrane

law (Gupta (2003), Pinacci and Drago (2012)), where the driving force is the difference in H_2 partial pressure on the membrane sides: the reactor side and the support side. The two partial pressures are indicated as $p_{H_2,rea}$ and $p_{H_2,0}$ respectively. The presence of the support, in turn, contributes to increasing the membrane-support interface pressure p_0, with respect to an unsupported membrane (Pinacci and Drago (2012)).

According to the Sieverts law, the H_2 permeated molar flow rate, $\tilde{w}_{H_2 M id}$, through the Pd membrane is

$$\tilde{w}_{H_2 M id} = (1-\theta_{Pd})\,(A_{Pd}/L_{Pd})\,Pe\,({p_{H_2,rea}}^n - {p_{H_2,0}}^n)\,, \quad (2)$$

where A_{Pd} and L_{Pd} are the membrane surface area (in a strip) and membrane thickness respectively; for simplicity, we take $A_{Pd} = A_{su}$ (the support surface area), since membrane thickness is negligible with respect to the support thickness (some μm against some mm). Pe $(mol/(m \cdot s \cdot Pa^n))$ is the so-called membrane permeability; it is a function of temperature T (K) and it can be described by the Arrhenius law

$$Pe = Pe_0 \cdot exp\,(-E_a/RT),$$

where E_a is the related activation energy (kJ/mol) and Pe_0 is the pre-exponential constant. Finally, H_2 partial pressure on the reactor side of the membrane is, of course, $p_{H_2,rea} = p_{rea} x_{H_2,rea}$, where $x_{H_2,rea}$ is H_2 molar fraction on the reactor side. Variable θ_{Pd} describes membrane poisoning by CO, which is adsorbed on the membrane surface and partially prevents H_2 permeation (see Bittanti et al. (2013) for a dynamic description of θ_{Pd}): calling θ_{Pd} the membrane surface fraction occupied by CO, the membrane permeation active area in the Sieverts equation is reduced by a factor $1-\theta_{Pd}$.

Some defects (see Section 4.1) may be present in the Pd layers, so that the overall flux through the membrane is the sum of the H_2 Sieverts flux, which is related to the permeation mechanism, and the flux of all gas species (including H_2) passing through the defects.

2.2 H_2 Molar Flow Rate across the Support

With reference to a H_2-N_2 binary mixture and assuming laminar flow, the H_2 molar flow rate across the membrane support, $\tilde{w}_{su}$, can be related to the pressure drop across

the support itself, $p_0 - p_L$, by the Blake-Kozeny equation (see Bird et al. (2002)):

$$\tilde{w}_{su} = \frac{g_0 A_{su} \bar{\rho} \cdot (p_0 - p_L)}{L_{su} \mu_{H_2 N_2} \overline{PM}}, g_0 = \frac{D_p^2 \varepsilon^3}{150(1-\varepsilon)^2}, \quad (3)$$

where the average molar weight $\overline{PM}$ of the binary mixture in the support, the average (mass) density in the support $\bar{\rho}$ and the binary mixture average viscosity $\mu_{H_2N_2}$ in the support are computed by weighting, respectively, H_2 and N_2 molar weights, the overall mass density and H_2 and N_2 viscosities by the H_2 and N_2 molar fractions on the two sides of the support, *i.e.* the Pd-support interface and the support sweep side.

2.3 N_2 Molar Conservation Equation in the Support

When N_2 is used as a sweep gas, a binary H_2-N_2 gaseous mixture, is present in the porous support, so N_2 molar conservation equation has to be included in the model. While H_2 actually flows across the support thickness, N_2 is stagnant there, *i.e.* N_2 total flux across the support is zero. In dynamic conditions, N_2 storage in the support has been considered; however, since the support thickness L_{su} is small, fast dynamics (of the order of fractions of a second) can be neglected, so N_2 molar conservation equation in each strip, along the radial coordinate r, reads as

$$\tilde{w}_{su} x_{N_2} - \tilde{\rho}_{su} D_{H_2N_2} A_{su} (\partial x_{N_2}/\partial r) = 0, \quad (4)$$

where $\tilde{w}_{su}$ $(kmol/s)$ is molar flow rate across the support, x_{N_2} nitrogen molar fraction in the binary mixture inside the support, $\tilde{\rho}_{su}$ $(kmol/m^3)$ gas molar density inside the support, $D_{H_2N_2}$ (m^2/s) the N_2-H_2 binary diffusion coefficient, A_{su} (m^2) the support surface area. Since the membrane is not permeable to N_2, at steady state $\tilde{w}_{su}$ coincides with the H_2 permeated molar flow rate.

Integrating (4) from $r = L_{su}$ to $r = 0$, H_2 partial pressure at the Pd-support interface can be derived:

$$p_{H_2,0} = p_0 x_{H_2,0} = p_0 (1 - x_{N_2,0}) = \\ = p_0 (1 - x_{N_2,L} exp(-\tilde{w}_{su} L_{su}/(\tilde{\rho}_{su} D_{H_2N_2} A_{su}))), \quad (5)$$

where $x_{H_2,0}$ and $x_{N_2,0}$ are hydrogen and nitrogen molar fraction, respectively, in the binary mixture at the Pd-support interface, while $x_{N_2,L}$ is nitrogen molar fraction in the binary mixture at the support-sweep gas interface.

2.4 Energy Conservation Equations

Two energy conservation equations, one for the membrane support and one for the Pd layer (see Bittanti et al. (2013)), are considered. The former accounts for the thermal exchange between the membrane support and the Pd layers, the thermal exchange between the support and the sweep gas, and the energy transport due to H_2 radial flux across the support. The latter accounts for the same thermal exchange between the support and the Pd layers, for that between the Pd layer and the porous medium in the reactor, and for the energy carried by permeated H_2.

3. REACTOR MODEL

The WGS reactor description adopted here (see Bittanti et al. (2008), Adams II and Barton (2009), Brunetti et al. (2007)) includes the energy and mass transport phenomena involving the feedgas stream and the catalytic porous medium (where CO is adsorbed/desorbed and the WGS reaction occurs), and mass and thermal exchanges with the supported membrane. The adopted Conservation Equations (CEs), *in each strip k*, are described in Bittanti et al. (2013), and they can be summed up as follows.

As for *mass* CEs, species i mole CE in the pellet gas and species i mole CE in the bulk gas, for $i = H_2O$, CO_2, CO, beside H_2 mole CE in the bulk and pellet volume (assuming a common average H_2 molar fraction for both volumes), have been adopted.

As for *chemical kinetics*, the WGS reaction dynamics are described by accounting for how fast and how much CO is adsorbed and desorbed on that surface and how fast and how much the adsorbed CO reacts in the direct and in the reverse direction (dependence of the reaction kinetic parameters on temperature is discussed in Bittanti et al. (2008)); the state variable is θ, the pellet pore surface fraction occupied by CO (in a strip; $1 - \theta$ will be the free surface fraction). Moreover, the net molar reaction rate $\dot{r}$ is a function of the i-th species molar concentration $(kmol/m^3)$ inside the pellet volume, where $i = H_2O, CO_2$, CO and H_2, and of θ, in each strip.

Energy CEs include, beside the already mentioned ones in the membrane metal support and in the membrane itself (Section 2.4), the one for the pellets, the one for the bulk gas and the one for the steel layer.

Momentum CEs are neglected: uniform pressure is assumed throughout the reactor, thanks to the fast dynamics of pressure control in the reference lab-scale facility.

4. SUPPORTED MEMBRANE PARAMETERS

The procedure adopted for membrane parameter identification is composed of two phases: in the former, experimental data with a single component (He or H_2) feedgas allow to identify the parameters describing the porous metal support permeation properties, membrane defects and the ideal membrane permeation properties; in the latter, the just obtained estimates, and experimental data with a binary, H_2-N_2, gas mixture are employed to analyse the influence of H_2-N_2 diffusion on membrane permeation. Here, identification is carried out for two membranes, the former 19.7 μm thick, the latter 30 μm thick.

We remind that, in all the experiments described below, the sweep gas pressure is kept to about the atmospheric pressure, more precisely $p_L = 100000\ Pa$. The notation $\Delta p_M := p_{rea} - p_0$, $\Delta p := p_0 - p_L$ and $p_{avg} := (p_0 + p_L)/2$ will be used in the following, respectively for pressure difference across the Pd layer, pressure difference across the support and average pressure in the support.

4.1 Tests with Single-Gas Feeds (He and H_2)

Identification of Parameter g_0 in the Blake-Kozeny Equation (3) Parameter g_0 describes the geometrical and material properties of the support. For the 19.7 μm membrane support, fourteen permeation tests, for the support only, have been carried out with He feed at room temperature (25 °C), yielding fourteen pairs $(p_{avg}, \tilde{w}_{He})$. For each test,

g_0 is computed from the viscous flow Blake-Kozeny equation (written for He) first:

$$\tilde{w}_{He} = (p_0 - p_L) \cdot (g_0/\mu_{He}) \cdot (A_{su}/L_{su}) \cdot p_{avg}/(RT), \quad (6)$$

with He viscosity evaluated as $\mu_{He} \simeq (0.4445 T_{He} + 188.56) \times 10^{-7} Pa{\cdot}s$, with T_{He} in $^\circ C$. Then, a linear fitting is found, as a function of Δp, from the computed values of g_0:

$$g_0 = a\Delta p + b = a(p_0 - p_L) + b. \quad (7)$$

The thus obtained values for a and b are $a = -3.5723 \times 10^{-21} m^2/Pa$ and $b = 5.4236 \times 10^{-15} m^2$. Comparing the values obtained for g_0 directly from (6) and from linear fitting (7), for each experimental test, one can see that (7) supplies a good approximation, so that (7) is used to compute g_0, in different operating conditions. For the 30 μm membrane support, the same values for a and b have been adopted, because it is identical to the 19.7 μm membrane support.

Identification of Membrane Defects Some defects may be present in the Pd layers, so that more H_2 crosses the membrane (and its support) than predicted by the ideal Sieverts law (2). Of course, in such a case other species can cross the membrane as well.

Let us consider tests with He gas feed for each of the two supported membranes. Helium does not permeate across the Pd lattice, of course, but there is a He viscous flow across the Pd layer driven by absolute pressure difference across Pd. For the 19.7 μm thick membrane, four sets of five H_2 tests each, at four different temperatures (310, 360, 380 and 400 °C), are available. For the 30 μm thick membrane, there are three sets of nine tests each, but all at temperature 400 °C. For both membranes, data pairs $(p_{He}, \tilde{w}_{He})$ have been employed in the following identification procedure:

- use (6) to describe He viscous flow across the supported membrane; replace g_0 in (6) by (7); then, for each test, replace in (6) the measured (molar) flow rate $\tilde{w}_{He}$ and the imposed pressure p_L: thus, compute the interface pressure p_0 and consequently $\Delta p_M = p_{He} - p_0$, falling across the Pd layer;
- from the computed p_0 and Δp_M values, fit the set of $(\Delta p_M, \tilde{w}_{He})$ pairs, for all temperatures, according to the Ergun equation (Bird et al. (2002))

$$\frac{\Delta p_M}{L_{Pd}} = k_l \frac{\mu_{He}}{\bar{\tilde{\rho}}_{He}} \frac{\tilde{w}_{He}}{A_{Pd}} + k_t \frac{PM_{He}}{\bar{\tilde{\rho}}_{He}} \left(\frac{\tilde{w}_{He}}{A_{Pd}}\right)^2, \quad (8)$$

where the average He molar density in the Pd layer is approximated as $\bar{\tilde{\rho}}_{He} = (p_{He} + p_0)/(2RT)$ and the uncertain parameters k_l and k_t are a laminar and a turbulent friction coefficient respectively. The estimated coefficients for the 19.7 μm membrane are $k_l = 2.0244 \times 10^{19} m^{-2}$ and $k_t = 2.4778 \times 10^{16} m^{-1}$, those for the 30 μm membrane are $k_l = 5.3693 \times 10^{18} m^{-2}$ and $k_t = 9.7504 \times 10^{15} m^{-1}$ (with an average relative error of the computed against the measured molar flow rate of 3.64% and 2.44% respectively for the two membranes).

Then, we consider H_2 membrane permeation tests, with their overall measured permeated flow rate $\tilde{w}_{H_2}$: for the 19.7 μm thick membrane, four sets of eight H_2 tests each, at four different temperatures (310, 360, 380 and 400 °C); for the 30 μm thick membrane, three sets of five tests each, at three different temperatures (314, 358 and 400 °C). For both membranes, data pairs $(p_{H_2}, \tilde{w}_{H_2})$ have been employed, together with coefficients k_l and k_t, to evaluate the H_2 flow rate through the membrane defects, $\tilde{w}_{H_2,def}$, as compared to $\tilde{w}_{H_2}$. To this aim, for each supported membrane start from the $\tilde{w}_{H_2}$ data and

- rewrite the Blake-Kozeny equation (6) for H_2 molar flow rate $\tilde{w}_{H_2}$ across the support, using (7) for g_0:

$$\tilde{w}_{H_2} = \frac{\Delta p}{L_{su}} \frac{a\Delta p + b}{\mu_{H_2}} \frac{(p_0 + p_L) A_{su}}{2RT}, \quad (9)$$

with $\mu_{H_2} \simeq (0.1771 T_{H_2} + 86.139) \times 10^{-7} Pa{\cdot}s$, T_{H_2} in $^\circ C$; thus, compute pressure p_0 and the pressure drop across Pd, *i.e.* $\Delta p_M = p_{H_2} - p_0$;
- rewrite (8) for H_2, *i.e.* for $\tilde{w}_{H_2,def}$:

$$\frac{\Delta p_M}{L_{Pd}} = k_l \frac{\mu_{H_2}}{\bar{\tilde{\rho}}_{H_2}} \frac{\tilde{w}_{H_2,def}}{A_{Pd}} + k_t \frac{PM_{H_2}}{\bar{\tilde{\rho}}_{H_2}} \left(\frac{\tilde{w}_{H_2,def}}{A_{Pd}}\right)^2. \quad (10)$$

Solve this equation and therefore find $\tilde{w}_{H_2,def}$.
- The ideal permeated flow rate, in the absence of defects, is therefore

$$\tilde{w}_{H_{2Mid}} = \tilde{w}_{H_2} - \tilde{w}_{H_2,def} \quad (11)$$

Numerical results show that $\tilde{w}_{H_2,def}$ amounts to few per cents only of the experimental flow rate $\tilde{w}_{H_2}$: about 2.29% for the 19.7 μm membrane, about 5.59% for the 30 μm membrane, in agreement with Pinacci and Drago (2012) and Pinacci et al. (2010). Therefore, in the subsequent Sieverts law identification, $\tilde{w}_{H_2,def}$ can be neglected.

Identification of the Membrane Ideal Permeation Parameters The ideal permeation features of each membrane, described by parameters Pe_0, E_a and n in Sievert's law (with $\theta_{Pd} = 0$), are now identified. Pe_0 and E_a are intrinsic values for a membrane, so they are independent of temperature. The obtained results are reported in Table 1, assuming membrane defects as negligible, *i.e.* $\tilde{w}_{H_2,def} = 0$; in parentheses, the results obtained considering defects are reported as well, for comparison: they are only slightly different from the previous ones, and the Sieverts molar flow rate is slightly smaller than the overall permeated one.

The adopted estimation procedure is as follows:

- at each temperature, compute n_{opt}, the optimal value of n, which supplies the maximal correlation coefficient for data $\left({p_{rea}}^n - {p_0}^n, \tilde{w}_{H_{2_M}}\right)$, with p_0 and $\tilde{w}_{H_{2_M}}$ computed from (9) and (11). Then, averaging n_{opt} with respect to temperature yields $\bar{n}_{19.7\mu m}$ and $\bar{n}_{30\mu m}$;
- for each temperature, find the linear regression from data $\left({p_{rea}}^{\bar{n}} - {p_0}^{\bar{n}}, \tilde{w}_{H_{2_M}}\right)$, since the slope of each straight line is $K_T = (A_{Pd}/L_{Pd})\, Pe_0 e^{-\frac{E_a}{RT}}$.
- obtain Pe_0 and E_a by regression from the set $(T_0/T, \ln K_T)$, with T_0 an arbitrary reference temperature (here, $T_0 = 298.15$ K).

4.2 Tests with Binary Mixtures on the Sweep Side

In the presence of N_2 as a sweep gas, the behaviour of the supported membrane is described by (2) (with $\theta_{Pd} = 0$),

(3) and (5). This last, in particular, describes how $p_{H_2,0}$ is influenced by N_2 which is present in the support beside H_2. The main parameter to be estimated in (5) is the diffusion coefficient $D_{H_2N_2}$. To this aim, we consider permeation tests with H_2 feedgas and N_2 sweep gas, at temperature 400 °C: for the 19.7 μm supported membrane, fifteen tests for each of four different N_2 sweep flow rates, namely 5, 25, 50 and 100 Nl/h; for the 30 μm supported membrane, eight tests with 50 Nl/h N_2 sweep molar flow rate.

The measured variables are the H_2 feed molar flow rate $\tilde{w}_{H_2,rea}$, the N_2 sweep molar flow rate $\tilde{w}_{N_2,L}$, the permeated H_2 molar flow rate $\tilde{w}_{H_2,L}$, the H_2 partial pressure $p_{H_2,rea}$, which coincides with total pressure p, on the reactor side, and the sweep pressure p_L; the N_2 average molar fraction in the sweep gas is computed by using the molar conservation equations for each component (H_2 and N_2) in the quasi-steady state assumption, namely it is approximated as $\bar{x}_{N_2,L} = [1 + \tilde{w}_{N_2,L}/(\tilde{w}_{N_2,L} + \tilde{w}_{H_2,L})]/2$. First of all, the values of these quantities obtained from the experiments have been employed in (2), (3) and (5), using, for the dependence of $D_{H_2N_2}$ on pressure and temperature, the Chapman-Enskog theory (Bird et al. (2002), page 526). Then, a correction factor k_D has been introduced: replacing $D_{H_2N_2}$ by $k_D D_{H_2N_2}$ in the model, a simple iterative procedure to minimize the error $E_{w_{H_2}}$ between the experimental (subscript S) permeated molar flow rate values and the corresponding values computed by the model (subscript C), *i.e.* $E_{w,H_2} := |(\tilde{w}_{H_2,S} - \tilde{w}_{H_2,C})/\tilde{w}_{H_2,S}|$, has yielded $k_{D_{19.7}} = 0.057$ and $k_{D_{30}} = 0.081$, with $E_{w,H_2,19.7} = 7.50\%$ and $E_{w,H_2,30} = 5.77\%$ (irrespectively of defects, since $D_{H_2N_2}$ does not depend on them). The correction factor is needed to take into account the effect of support material properties such as porosity and tortuosity.

The obtained model appears as physically sound. For instance, the computed Pd-support interface pressure p_0 is higher in the presence of the sweep gas than in the absence of the sweep gas, because $\tilde{w}_{H_2}$ is higher, as shown in (3); besides, the difference between p_0 values in the two cases increases if $p_{H_2,rea}$ is increased.

5. DYNAMIC SIMULATION RESULTS

The overall membrane reactor dynamic model has been implemented with an object-oriented approach, by means of a main Dymola block connected to Matlab-Simulink blocks for easier input-output management.

Table 1. n_{opt}, E_a and Pe_0 estimates neglecting defects (in parentheses, considering defects)

T (°C)	$n_{opt,19.7\mu m}$	T (°C)	$n_{opt,30\mu m}$
310	0.6483 (0.6325)	314	0.6061 (0.5745)
360	0.6668 (0.6538)	358	0.5618 (0.5336)
380	0.6731 (0.6610)	400	0.5924 (0.5076)
400	0.7124 (0.7012)		
	$\bar{n}_{19.7\mu m} = 0.6752$ (0.6621)		$\bar{n}_{30\mu m} = 0.5658$ (0.5386)
	19.7μm membr.		30μm membr.
E_a	10.469 kJ/mol (10.811 kJ/mol)	E_a	18.388 kJ/mol (19.448 kJ/mol)
Pe_0	$\frac{6.131\times10^{-9}mol}{m\cdot s\cdot Pa^{0.675}}$ $\left(\frac{7.742\times10^{-9}mol}{m\cdot s\cdot Pa^{0.662}}\right)$	Pe_0	$\frac{1.182\times10^{-7}mol}{m\cdot s\cdot Pa^{0.566}}$ $\left(\frac{2.045\times10^{-7}mol}{m\cdot s\cdot Pa^{0.539}}\right)$

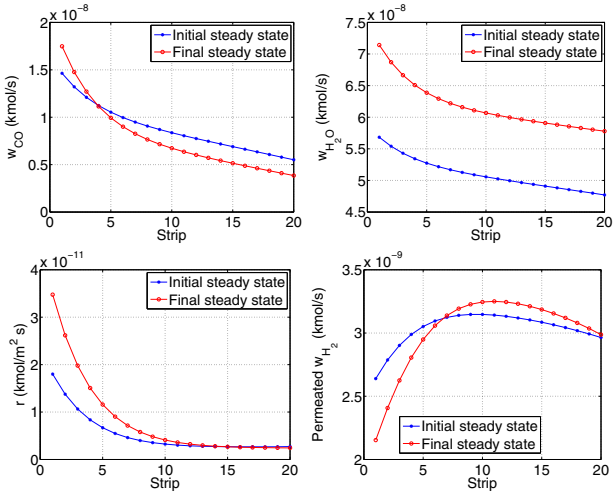

Fig. 2. Simulation results: steady-state variables, before and after the step perturbation

Simulation results are now reported, starting from the same steady-state conditions as an experimental test carried out in the described facility on a lab-scale shift reactor operating with the 30μm membrane inside. The test, which was also employed to estimate the palladium poisoning by CO (see also Bittanti et al. (2013)), is characterized by these process variables: $\tilde{w}_{feed}$ =17.71 Nl/h; p_{feed} = 310000 Pa; T = 400 °C; molar fractions at the reactor inlet: $x_{H_2O} = 0.271$, $x_{CO} = 0.076$, $x_{CO_2} = 0.237$, $x_{H_2} = 0.416$; 50 Nl/h N_2 sweep molar flow rate. At steady state, the measured molar fractions at the reactor outlet were $x_{H_2O} = 0.2975$, $x_{CO} = 0.0321$, $x_{CO_2} = 0.3947$, $x_{H_2} = 0.2754$ and the measured overall permeated H_2 molar flow rate was 5.8414×10^{-8} kmol/s. The reactor is 9.5 cm long, with the outer radius $r_{ext} = 1$ cm and the inner radius $r_{int} = 0.5$ cm; N has been taken as 20.

We now assume a step variation of the reactor inlet composition: the inlet CO and H_2O molar flow rates are increased by 27.8% and the inlet CO_2 and H_2 molar flow rates are decreased by 14.8%, at the same time, keeping the initial overall molar flow rate $\tilde{w}_{feed}$ constant.

The *steady-state* conditions before and after the step perturbation are compared in Fig. 2, in terms of bulk molar flow rates, shift reaction rate $\dot{r}$ and permeated H_2 molar flow rate along the reactor strips. As for the initial steady state, as expected, CO is converted into CO_2, so CO and H_2O molar flow rates decrease from the reactor inlet to the outlet. H_2 molar flow rate (not shown, for brevity) decreases, instead, because it is removed from the bulk gas thanks to the membrane: indeed, the H_2 permeated molar flow rate has an overall increasing trend from the inlet to the outlet of the reactor. For the new steady state after the transient, the qualitative behaviour along the strips is the same. The final steady-state reaction rate along the reactor is higher than the initial one, since the inlet reactants have been increased and the inlet products have been decreased; accordingly, CO final molar flow rates are below the initial ones almost throughout the reactor, notwithstanding the increment supplied at the inlet.

Figure 3 shows some *transient* results along the membrane reactor, for seven of the simulated twenty strips to enhance

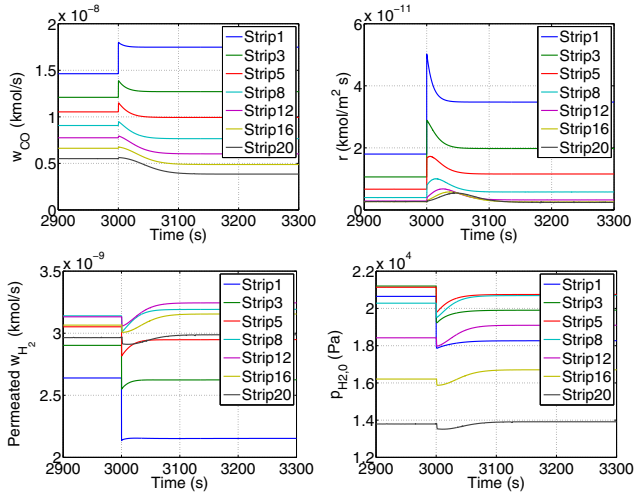

Fig. 3. Simulation results: variable transients

readability. The inlet steps in molar flow rates have a clear direct effect on all molar flow rates and on $p_{H_2,0}$ in the first strip; however, the simultaneous reactants increase and products decrease imposed at the inlet enhance the direct shift reaction, increasing reaction rate and CO conversion (from 66.52% to 81.75% between the two steady states): thus, *e.g.*, CO has a decreasing transient after the step, and $p_{H_2,0}$ decreases less and less towards the end of the reactor, so that the permeated H_2 molar flow rate has an increasing trend after the step. The total membrane permeated flow rate at the end of the transient is 6.0305×10^{-8} *kmol/s*, *i.e.* a little lower than the initial one, since H_2 is decreased at the inlet and it has an overall decreasing transient almost throughout the reactor.

6. CONCLUSION

The Dymola membrane model can be proposed as a design tool for prototype membrane WGS reactors, and also as a starting point for their control design. For instance, in order to avoid reverse H_2 permeation across the membrane, especially at the reactor inlet (the feedgas and the sweep gas flow in counter current), it is necessary to control the sweep gas flow rate adequately, since it contributes, together with the inlet composition, to determine the H_2 profile along the reactor. To this purpose, further developments are advisable. In particular, palladium poisoning by CO and also by CO_2 has to be studied, for example starting from experiments such as those described in Liguori et al. (2012). Secondly, parameter estimation could be refined by an incremental identification approach (Brendel et al. (2006)), which would make systematic the heuristic procedure adopted so far to identify a parameter after another.

Finally, note that, although this work refers to a WGS reactor in particular, the same general approach can be followed for other kinds of reactors where a Pd membrane can be placed to work, *e.g.* those for methane steam reforming (Ghouse and Adams II (2013)).

REFERENCES

Adams II, T.A. and Barton, P.I. (2009). A dynamic two-dimensional heterogeneous model for water gas shift reactors. *Int. J. Hydrogen Energ.*, 34(21), 8877–8891.

Augustine, A.S., Ma, Y.H., and Kazantzis, N.K. (2011). High pressure palladium membrane reactor for the high temperature water-gas shift reaction. *Int. J. Hydrogen Energ.*, 36(9), 5350–5360.

Bird, R.B., Stewart, W.E., and Lightfoot, E.N. (2002). *Transport Phenomena, 2nd Edition*. John Wiley & Sons, USA.

Bittanti, S., Bolzani, L., Canevese, S., De Marco, A., Drago, F., and Pinacci, P. (2013). Modelling for a palladium membrane water-gas shift reactor. In *Prepr. of the 2nd IFAC ICPS*. Cluj-Napoca, Romania.

Bittanti, S., Canevese, S., De Marco, A., Prandoni, V., and Serrau, D. (2008). Towards clean-coal control technologies: modelling conversion of carbon oxide into hydrogen by a shift reactor. In *Proc. of the 17th IFAC World Congress*. Seoul, Korea.

Brendel, M., Bonvin, D., and Marquardt, W. (2006). Incremental identification of kinetic models for homogeneous reaction systems. *Chem. Eng. Sci.*, 61(16), 5404–5420.

Brunetti, A., Caravella, A., Barbieri, G., and Drioli, E. (2007). Simulation study of water gas shift reaction in a membrane reactor. *J. Membrane Sci.*, 306(1-2), 329–340.

Buxbaum, R.E. and Kinney, A.B. (1996). Hydrogen transport through tubular membranes of palladium-coated tantalum and niobium. *Ind. Eng. Chem. Res.*, 35(2), 530–537.

Gallucci, F., Fernandez, E., Corengia, P., and van Sint Annaland, M. (2013). Recent advances on membranes and membrane reactors for hydrogen production. *Chem. Eng. Sci.*, 92, 40–66.

Ghouse, J.H. and Adams II, T.A. (2013). A multi-scale dynamic two-dimensional heterogeneous model for catalytic steam methane reforming reactors. *Int. J. Hydrogen Energ.*, 38(24), 9984 –9999.

Gupta, C.K. (2003). *Chemical Metallurgy: Principles and Practice*. Wiley-VCH, Germany.

Kikuchi, E. (1995). Palladium/ceramic membranes for selective hydrogen permeation and their application to membrane reactors. *Catal. Today*, 25(3-4), 333–337.

Liguori, S., Pinacci, P., Seelam, P.K., Keiski, R., Drago, F., Calabrò, V., Basile, A., and Iulianelli, A. (2012). Performance of a Pd/PSS membrane reactor to produce high purity hydrogen via WGS reaction. *Catal. Today*, 193(1), 87–94.

Lu, G.Q., Diniz da Costa, J.C., Duke, M., Giessler, S., Socolow, R., Williams, R.H., and Kreutz, T. (2007). Inorganic membranes for hydrogen production and purification: A critical review and perspective. *J. Colloid Interf. Sci.*, 314(2), 589–603.

Pinacci, P., Broglia, M., Valli, C., Capannelli, G., and Comite, A. (2010). Evaluation of the water gas shift reaction in a palladium membrane reactor. *Catal. Today*, 156(3-4), 166–172.

Pinacci, P. and Drago, F. (2012). Influence of the support on permeation of palladium composite membranes in presence of sweep gas. *Catal. Today*, 193(1), 186–193.

Shirasaki, Y., Tsuneki, T., Ota, Y., Yasuda, I., Tachibana, S., Nakajima, H., and Kobayashi, K. (2009). Development of membrane reformer system for highly efficient hydrogen production from natural gas. *Int. J. Hydrogen Energ.*, 34(10), 4482–4487.